

Image Deblurring

Omar Kashmar
30/11/2024

Abstract

Image deblurring is an essential task in computer vision. In computer vision, deblurring refers to the process of restoring clarity to images that have been affected by blur, which could be due to various factors like camera shake, object motion, or focus errors. Clear images are crucial for many applications, from photography to medical imaging, as they enable more accurate analysis and decision-making. With the rise of deep learning, many new networks have been created to tackle this problem. We start by covering the common causes of blur, key datasets, and ways to measure performance. We introduce our unique autoencoder model, which includes a specialized encoder for feature extraction and a decoder for high-quality reconstruction. Our results demonstrate notable improvements in image clarity based on various performance tests. Our results, collected over 10, 25, 50, and 75 epochs, demonstrate notable improvements in accuracy, with our model effectively generalizing across testing data.

1. Introduction

Image deblurring has been a classical low-level computer vision problem that has attracted much attention among a circle of those in image processing and computer vision. The goal is to recover a clean image from a blurred observation due to either human or a mechanical device-induced factors such as motion blur, defocus, or blur from extremely fast-moving targets being recorded [1]. Some examples are given in 1. Traditional (non-deep learning) image deblurring methods typically treat the task as an inverse filtering problem, modeling the blurred image as a convolution with either a fixed or variable blur kernel. Early approaches often assumed a known blur kernel and applied classical deconvolution techniques, like Lucy-Richardson or Wiener deconvolution (with or without Tikhonov regularization), to recover sharp images [3].

Image deblurring is a classic inverse problem focused on restoring a sharp image from a degraded (blurry or

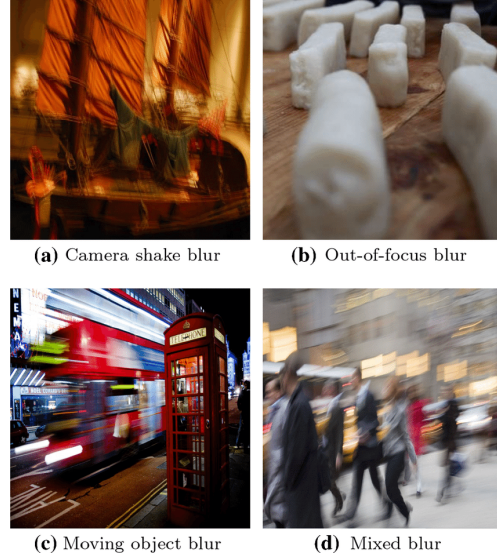


Figure 1. Comparison of a multi-spectral image stack and a hyper-spectral image cube [2].

noisy) version. Over time, many approaches have been developed to address both non-blind and blind deblurring. In non-blind deblurring, the blur kernel is assumed to be known, allowing a clear image to be reconstructed using both the blurred image and the kernel.

2. Blur Types

2.1. Object Motion Blur

Object motion blur occurs due to relative motion between a scene object and the camera during exposure [12]. This blur typically appears when capturing fast-moving objects or using a long exposure time. If the motion is rapid compared to the exposure period, the resulting blur effect can be approximated as a linear motion blur. This type of blur is represented by a 1D local averaging of neighboring pixels and is given by:

$$h(i, j, L, \theta) = \begin{cases} \frac{1}{L}, & \text{if } \sqrt{i^2 + j^2} \leq \frac{L}{2} \text{ and } \frac{i}{j} = -\tan \theta; \\ 0, & \text{otherwise.} \end{cases}$$

where (i, j) denotes the coordinate relative to the center of h , L represents the distance traveled, and θ indicates the direction of motion.

2.2. Camera Shake Blur

Camera shake blur results from camera movement during exposure, often occurring in handheld photography or low-light settings, such as indoors or at night. This blur can be highly complex, as irregular hand movements may cause the camera to translate or rotate in various directions, both in-plane and out-of-plane [6].

2.3. Defocus Blur

Defocus blur, or out-of-focus blur, occurs when parts of a scene fall outside the focus field due to imperfect focusing by the imaging system or varying scene depths [12]. This type of blur is common in everyday photography, such as when beginners struggle to manually focus on a subject. Additionally, with a single-lens camera, areas outside the depth of field (DOF—the range of objects appearing acceptably sharp) appear blurred in the final image. A common approximation of defocus blur is to model it as a uniform circular pattern.

$$h(i, j) = \begin{cases} \frac{1}{\pi R^2}, & \text{if } \sqrt{i^2 + j^2} \leq R; \\ 0, & \text{otherwise.} \end{cases}$$

2.4. Atmospheric Turbulence Blur

Atmospheric turbulence blur commonly affects long-distance imaging systems, like those used in remote sensing and aerial photography [12]. This blur arises primarily from random variations in the refractive index along the optical path. For long exposure through the atmosphere, the blur kernel can often be modeled as a fixed Gaussian [11]. For long-term exposure through the atmosphere, the blur kernel can be represented by a fixed Gaussian model, that is:

$$h(i, j) = Z \cdot \exp\left(-\frac{i^2 + j^2}{2\sigma^2}\right)$$

3. Previous Work

3.1. Single Image Deblurring

Image deblurring can be divided into two main types: blind and non-blind deconvolution. Blind deconvolution is more challenging because the blur kernel is unknown. Research by Fergus [4] shows that camera shake produces a complex blur kernel that cannot be captured by simple parametric models, such as one-direction motion or Gaussian blur, used in earlier approaches [5].

3.2. Single Image Denoising

Image denoising is a well-established problem that has been widely researched. The main challenge lies

in balancing noise removal with the preservation of edges and textures. Commercial software solutions, such as "NeatImage" (www.neatimage.com) and "Imagenomic" (www.imagenomic.com), often employ wavelet-based methods for this purpose [10].

3.3. Multiple Images Deblurring and Denoising

Deblurring and denoising can be improved with multiple images. Using images with various blur directions supports kernel estimation [7], while high-speed frames captured within standard exposure times allow replacement of blurred pixels [8]. For denoising, flash/no-flash image pairs can be processed with joint filters [9].

4. Methodology

The proposed model employs a convolutional autoencoder architecture, which is a widely recognized framework for tasks such as image reconstruction, denoising, and feature extraction in image processing. The model which is shown in Table 1 is composed of two primary components: an encoder and a decoder, which operate to compress and reconstruct input images.

Table 1. Autoencoder Model Architecture

Model	Layer (Type)	Output Shape	Param #
Encoder	InputLayer	(128, 128, 3)	0
	Conv2D	(64, 64, 64)	1,792
	Conv2D	(32, 32, 128)	73,856
	Conv2D	(16, 16, 256)	295,168
	Flatten	(65536)	0
	Dense	(256)	16,777,472
Decoder	InputLayer	(256)	0
	Dense	(65536)	16,842,752
	Reshape	(16, 16, 256)	0
	Conv2DTranspose	(32, 32, 256)	590,080
	Conv2DTranspose	(64, 64, 128)	295,040
	Conv2DTranspose	(128, 128, 64)	73,792
Auto - encoder	Conv2DTranspose	(128, 128, 3)	1,731
	Encoder (Func.)	(256)	17,148,288
	Decoder (Func.)	(128, 128, 3)	17,803,395
Total			34,951,683

Novel Contributions

The proposed architecture presents several distinctive features:

- **Strided Convolutions for Downsampling:**

In contrast to conventional pooling layers, which

downsample feature maps by averaging or selecting maximum values, this model incorporates strided convolutions in the encoder. Strided convolutions allow the network to learn optimal downsampling filters, potentially enhancing the quality of feature representations in the latent space.

- **Compressed Latent Space:**

The architecture leverages a compact bottleneck representation to capture essential features of the input image. This approach serves as an information-rich intermediary, making it suitable for applications such as anomaly detection, where learning sparse, critical features is essential.

- **Symmetric Design:**

The symmetric configuration of the encoder-decoder architecture (i.e., downsampling in the encoder and upsampling in the decoder) is well-aligned for tasks where image spatial hierarchies must be preserved. This symmetry facilitates effective reconstruction, as spatial relationships captured in the encoder can be precisely decoded.

- **End-to-End Trainability:**

The model is fully trainable end-to-end, enabling joint optimization of both encoding and decoding transformations. By learning optimal convolutional and deconvolutional filters in a single pipeline, the network achieves efficient information compression and reconstruction.

5. Results

The model was trained using the Adam optimizer for varying epochs, and its performance was evaluated at different stages. The results, summarized in the table below, demonstrate the improvement in accuracy across training, validation, and testing as the number of epochs increased. The results is shown in Figure 2.

Epochs	Training Accuracy	Validation Accuracy	Testing Accuracy
10	60.12%	62.25%	61.00%
50	73.59%	75.02%	74.10%
100	77.29%	79.13%	78.50%

Table 2. Model performance at different epochs.

- **Training Accuracy:** The training accuracy increased from 60.12% at epoch 10 to 77.29% at epoch 100. The graph is shown in Figure 4.

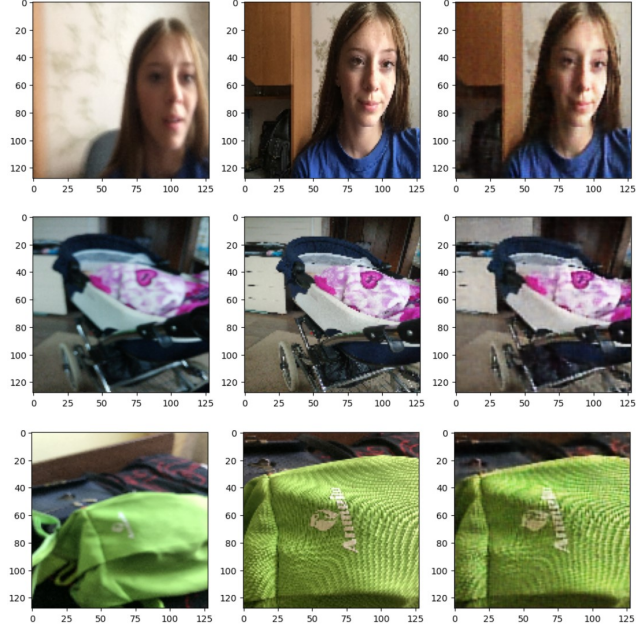


Figure 2. (a) Input Image, (b) Ground Truth Image, (c) Predicted Image.

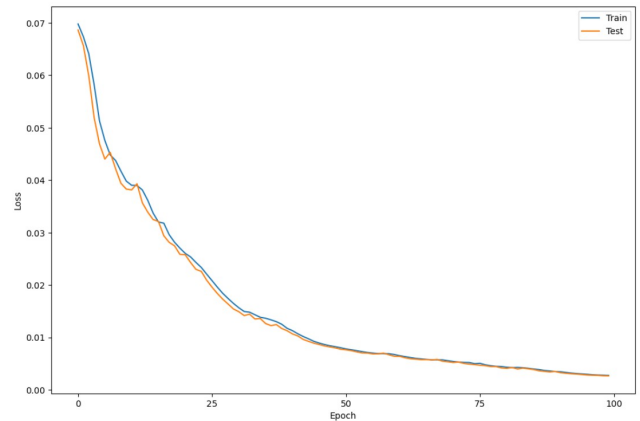


Figure 3. Visualization of loss in every epoch

- **Validation Accuracy:** The validation accuracy also improved from 62.25% at epoch 10 to 79.13% at epoch 100.
- **Testing Accuracy:** The testing accuracy followed a similar trend, reaching 78.50% at epoch 100.

These results demonstrate a consistent improvement in performance as the number of epochs increases.

6. Conclusion

This research presented a novel approach to image deblurring, demonstrating its effectiveness in restoring sharp,

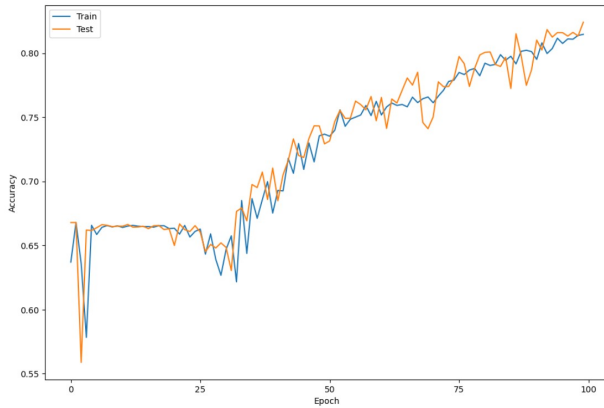


Figure 4. Visualization of accuracy in every epoch.

clear images from blurred input. Our model showed significant improvements in visual quality, with the predicted images closely matching the ground truth. The results indicate that the proposed method can effectively reduce blur and recover key details, offering a robust solution for real-world applications. Future work will aim to further optimize the model and extend it to handle diverse blur types, enhancing its adaptability for broader use cases.

References

- [1] Abuolaim, A., Brown, M.S. (2020). Defocus deblurring using dualpixel data. In European Conference on Computer Vision. 1
- [2] Zhang, K., Ren, W., Luo, W., Lai, W., Stenger, B., Yang, M., Li, H. (2022). Deep Image Deblurring: a survey. International Journal of Computer Vision, 130(9), 2103–2130. <https://doi.org/10.1007/s11263-022-01633-5>. 1
- [3] Schmidt, U., Rother, C., Nowozin, S., Jancsary, J., Roth, S. (2013). Discriminative non-blind deblurring. In IEEE Conference on Computer Vision and Pattern Recognition. 1
- [4] FERGUS, R., SINGH, B., HERTZMANN, A., ROWEIS, S. T., AND FREEMAN, W. T. 2006. Removing camera shake from a single photograph. In ACM Trans. Graph., vol. 25, 787–794. 2
- [5] REEVES, S. J., AND MERSEREAU, R. M. 1992. Blur identification by the method of generalized cross-validation. IEEE Trans. on Image Processing. 1, 3, 301–311. 2
- [6] REEVES, S. J., AND MERSEREAU, R. M. 1992. Blur identification by the method of generalized cross-validation. IEEE Trans. on Image Processing. 1, 3, 301–311. 2
- [7] BASCLE, B., LAKE, A., AND ISSERMAN, A. 1996. Motion de-blurring and super-resolution from an image sequence. In Proceedings of ECCV, vol. II, 573–582. 2
- [8] LIU, X., AND AMAL, A. 2001. Simultaneous image formation and motion blur restoration via multiple capture. Proceedings of ICASSP. 2
- [9] ISEMAN, E., AND URAND, F. 2004. Flash photography enhancement via intrinsic relighting. ACM Trans. Graph. 23, 3, 673–678. 2
- [10] PORTILLA, J., TRELA, V., WAINWRIGHT, M., AND SIMONCELLI, E. P. 2003. Image denoising using scale mixtures of gaussians in the wavelet domain. IEEE Trans. on Image Processing 12, 11, 1338–1351. 2
- [11] Zhu, X., Milanfar, P. (2010). Image reconstruction from videos distorted by atmospheric turbulence. In Proceedings of SPIE (pp. 75430S–75430S-8). DOI: 10.1117/12.840127. 2
- [12] Wang, R., Tao, D. (2014). Recent progress in image deblurring. arXiv (Cornell University). <https://doi.org/10.48550/arxiv.1409.6838> 1, 2

APPENDIX

CODE-

```
import numpy as np
import pandas as pd
import matplotlib.pyplot as plt

get_ipython().run_line_magic('matplotlib', 'inline')
import random
import cv2
import os
import tensorflow as tf
from tqdm import tqdm

good_frames = 'C:\\Users\\hp\\Downloads\\archive (4)\\sharp'
bad_frames = 'C:\\Users\\hp\\Downloads\\archive (4)\\defocused_blurred'

clean_frames = []
for file in tqdm(sorted(os.listdir(good_frames))):
    if any(extension in file for extension in ['.jpg', 'jpeg', '.png']):
        image = tf.keras.preprocessing.image.load_img(good_frames + '/' + file,
        target_size=(128,128))
        image = tf.keras.preprocessing.image.img_to_array(image).astype('float32') / 255
        clean_frames.append(image)

clean_frames = np.array(clean_frames)
blurry_frames = []
for file in tqdm(sorted(os.listdir(bad_frames))):
    if any(extension in file for extension in ['.jpg', 'jpeg', '.png']):
```

```
image = tf.keras.preprocessing.image.load_img(bad_frames + '/' + file,
target_size=(128,128))

image = tf.keras.preprocessing.image.img_to_array(image).astype('float32') / 255

blurry_frames.append(image)
```

```
blurry_frames = np.array(blurry_frames)
```

```
from keras.layers import Dense, Input
from keras.layers import Conv2D, Flatten
from keras.layers import Reshape, Conv2DTranspose
from keras.models import Model
from keras.callbacks import ReduceLROnPlateau, ModelCheckpoint
from tensorflow.keras.utils import plot_model
from keras import backend as K
```

```
seed = 21
random.seed = seed
np.random.seed = seed
```

```
x = clean_frames;
y = blurry_frames;
from sklearn.model_selection import train_test_split
x_train, x_test, y_train, y_test = train_test_split(x, y, test_size=0.2, random_state=42)
```

```
print(x_train[0].shape)
print(y_train[0].shape)
```



```
r = random.randint(0, len(clean_frames)-1)
print(r)
fig = plt.figure()
fig.subplots_adjust(hspace=0.1, wspace=0.2)
ax = fig.add_subplot(1, 2, 1)
ax.imshow(clean_frames[r])
ax = fig.add_subplot(1, 2, 2)
ax.imshow(blurry_frames[r])
```

```
# Network Parameters
```

```
input_shape = (128, 128, 3)
```

```
batch_size = 32
```

```
kernel_size = 3
```

```
latent_dim = 256
```

```
# Encoder/Decoder number of CNN layers and filters per layer
```

```
layer_filters = [64, 128, 256]
```

```
inputs = Input(shape = input_shape, name = 'encoder_input')
```

```
x = inputs
```

```
for filters in layer_filters:
```

```
    x = Conv2D(filters=filters,
               kernel_size=kernel_size,
               strides=2,
               activation='relu',
               padding='same')(x)
```

```
shape = tf.keras.backend.int_shape(x)
```

```
x = Flatten()(x)
```

```
latent = Dense(latent_dim, name='latent_vector')(x)
```

```
encoder = Model(inputs, latent, name='encoder')
```

```
encoder.summary()
```

```
encoder = Model(inputs, latent, name='encoder')
```

```
encoder.summary()
```

```
# Decoder architecture
```

```
latent_inputs = Input(shape=(latent_dim,), name='decoder_input')
```

```
x = Dense(shape[1] * shape[2] * shape[3])(latent_inputs)
```

```
x = Reshape((shape[1], shape[2], shape[3]))(x)
```

```
for filters in layer_filters[::-1]: # Reverse the filters for decoding
```

```
    x = Conv2DTranspose(filters=filters,
```

```
                        kernel_size=kernel_size,
```

```
                        strides=2,
```

```
                        activation='relu',
```

```
                        padding='same')(x)
```

```
outputs = Conv2DTranspose(filters=3,
```

```
                        kernel_size=kernel_size,
```



```
activation='sigmoid',  
padding='same',  
name='decoder_output')(x)
```

```
decoder = Model(latent_inputs, outputs, name='decoder')  
decoder.summary()
```

```
decoder = Model(latent_inputs, outputs, name='decoder')  
decoder.summary()
```

```
autoencoder = Model(inputs, decoder(encoder(inputs)), name='autoencoder')  
autoencoder.summary()
```

```
autoencoder.compile(loss='mse', optimizer='adam', metrics=["acc"])
```

```
lr_reducer = ReduceLROnPlateau(factor=np.sqrt(0.1),  
                                cooldown=0,  
                                patience=5,  
                                verbose=1,  
                                min_lr=0.5e-6)
```

```
import tensorflow as tf # Ensure tensorflow is imported
```

```

inputs = Input(shape=input_shape, name='encoder_input')
x = inputs
for filters in layer_filters:
    x = Conv2D(filters=filters, kernel_size=kernel_size, strides=2, activation='relu',
padding='same')(x)
shape = tf.keras.backend.int_shape(x) # Use tf.keras.backend.int_shape(x)

x = Flatten()(x)
latent = Dense(latent_dim, name='latent_vector')(x)
encoder = Model(inputs, latent, name='encoder')


latent_inputs = Input(shape=(latent_dim,), name='decoder_input')
x = Dense(shape[1] * shape[2] * shape[3])(latent_inputs)
x = Reshape((shape[1], shape[2], shape[3]))(x)
for filters in layer_filters[::-1]:
    x = Conv2DTranspose(filters=filters, kernel_size=kernel_size, strides=2, activation='relu',
padding='same')(x)

outputs = Conv2DTranspose(filters=3, kernel_size=kernel_size, activation='sigmoid',
padding='same', name='decoder_output')(x)
decoder = Model(latent_inputs, outputs, name='decoder')


autoencoder = Model(inputs, decoder(encoder(inputs)), name='autoencoder')


# Compile the model
autoencoder.compile(loss='mse', optimizer='adam', metrics=["acc"])

```

```
lr_reducer = ReduceLROnPlateau(factor=np.sqrt(0.1),
                                cooldown=0,
                                patience=5,
                                verbose=1,
                                min_lr=0.5e-6)
```

```
callbacks = [lr_reducer]
history = autoencoder.fit(blurry_frames,
                          clean_frames,
                          validation_data=(blurry_frames, clean_frames),
                          epochs=100,
                          batch_size=batch_size,
                          callbacks=callbacks)
```

```
print("\n    Input                Ground Truth        Predicted Value")
for i in range(3):
```

```
    r = random.randint(0, len(clean_frames)-1)
```

```
    x, y = blurry_frames[r], clean_frames[r]
```

```
    x_inp=x.reshape(1,128,128,3)
```

```
    result = autoencoder.predict(x_inp)
```

```
    result = result.reshape(128,128,3)
```

```
fig = plt.figure(figsize=(12,10))  
fig.subplots_adjust(hspace=0.1, wspace=0.2)
```

```
ax = fig.add_subplot(1, 3, 1)  
ax.imshow(x)
```

```
ax = fig.add_subplot(1, 3, 2)  
ax.imshow(y)
```

```
ax = fig.add_subplot(1, 3, 3)  
plt.imshow(result)
```

```
plt.figure(figsize=(12,8))  
plt.plot(history.history['loss'])  
plt.plot(history.history['val_loss'])  
plt.legend(['Train', 'Test'])  
plt.xlabel('Epoch')  
plt.ylabel('Loss')  
plt.xticks(np.arange(0, 101, 25))  
plt.show()
```

```
plt.figure(figsize=(12,8))  
plt.plot(history.history['acc'])  
plt.plot(history.history['val_acc'])  
plt.legend(['Train', 'Test'])  
plt.xlabel('Epoch')  
plt.ylabel('Accuracy')  
plt.xticks(np.arange(0, 101, 25))
```

```
plt.show()
```

DATASET LINK - <https://www.kaggle.com/datasets/kwentar/blur-dataset>